Charge Fractions and Excited-Atom Populations of 8–100 keV Deuterium Beams Emerging from Solid Films of C, Mg, Nb, and Au[†]

Klaus H. Berkner, Isaac Bornstein, Robert V. Pyle, and J. Warren Stearns

Lawrence Berkeley Laboratory, University of California, Berkeley, California 94720

(Received 20 March 1972)

Charge-state fractions and yields of highly excited deuterium atoms produced by electron capture when 8–100-keV deuterons emerge from C, Mg, Nb, and Au surfaces deposited on thin carbon foils under high-vacuum conditions are reported. Atoms with principal quantum number $n = 6$ were detected with an optical technique; atoms in the levels $n \approx 12$ to 18 were detected by ionizing them in a strong electric field. Changes with time after evaporation, presumably due to contamination of the surfaces, were observed. The experimental results are compared with available theoretical estimates. Solid and vapor targets are compared for Mg.

I. INTRODUCTION

A large amount of experimental and theoretical work on charge transfer in gases and vapors has been reported in the literature. Very little quantitative data is available concerning electron capture by hydrogen ions at solid surfaces, although a great deal of beam-foil interaction work concerned with spectroscopy and other aspects of atomic physics is currently being published.[1]

In the present work we report measurements of the charge fractions and excited-atom populations of 8–100-keV deuterium beams emerging from freshly deposited solid films. The work of relevance to the present paper probably started with the experiments of Phillips,[2] who measured charge-state fractions of the beam issuing from a foil freshly coated with various materials under moderately good vacuum conditions (approximately 10^{-6} Torr). Phillips showed that the fractions in various charge states changed with time after the material was deposited, all materials eventually giving about the same fractions, presumably due to surface contamination. Sweetman *et al.*[3] measured the excited-state yield of 20–100-keV H^0 atoms in the level $n = 11$ from a carbon foil, and found that it exceeded the yield from a hydrogen gas target. It was this favorable yield of excited-state atoms that provided the motivation for the present study of foils as a charge-exchange medium.

The purpose of the present experiment was to repeat Phillips's charge-fraction measurements under better vacuum conditions and to simultaneously measure the yield of excited states in the neutral component. Since Phillips showed that only the exit surface of a foil is important for electron capture, we used thin carbon foils as substrates and evaporated the materials to be studied on the exit surface under high-vacuum conditions ($< 10^{-8}$ Torr).

II. THEORETICAL BACKGROUND

In the energy range of interest here, electron capture by protons colliding with single atoms has been described fairly well by theoretical treatments that give both the total capture cross sections and partial cross sections for capture into any substate. This is most straightforward for collisions with hydrogen atoms, but experience has shown that calculations, based on the first Born approximation, can be adjusted by empirically based recipes to yield good results for collisions with any atom.[4] Much of this work, with emphasis on capture into highly excited states, has been carried out by Hiskes.[5]

The theoretical situation is much worse for the case of electron capture from condensed materials, perhaps because of the greater difficulty of describing the interaction of the proton with a lattice rather than with a single atom, and perhaps because of the paucity of experimental results for comparison with predictions. Of the papers that have been published on this topic in recent times,[6-10] only three give semiquantitative results.[6-8]

In the first paper, Yavlinskii, Trubnikov, and Elesin[6] have calculated the recombination that takes place at the surface of a metal foil (Debye shielding is assumed to prevent capture in the interior of the metal), treating the capture in the electron gas at the surface as a recombination process. The calculation was carried out in the two limits that the proton speed v_p is much larger than or much smaller than the speed v_0 of an electron at the Fermi surface. In terms of the conduction electron density within the metal, $n_0 (\mathrm{cm}^{-3})$, and the kinetic energy of the proton, $E_p (\mathrm{keV})$, they found that the fraction of the total beam emerging as protons is given in the two limits by

$$v_p \ll v_0: \quad F^+ = \exp[-(136/E_p)^{1/2} (n_0/10^{22})^{1/6}], \quad (1)$$

$$v_p \gg v_0: \quad F^+ = \exp[-(6.5/E_p)(n_0/10^{22})^{1/2}]. \quad (2)$$

The experiments reported to date fall approximately in the range $1 < v_p/v_0 < 10$. If we neglect the formation of negative ions, we see from the above expressions that the neutral fraction, $F_0 = 1 - F^+$, is predicted to be approximately unity at low energies, in agreement with experiment, and to drop off at high energy as $1/E_p$, which is much slower than is observed experimentally.[2]

In a later paper, Trubnikov and Yavlinskii considered the case of tunnel recombination near the surface of a metal foil.[7] The calculation was again carried out in two limits: The "fixed-ion approximation" (essentially the assumption that $v_p \ll v_0$) yields the result that almost all of the neutral atoms are produced in the $n = 2$ and $n = 3$ levels. Using time-dependent perturbation theory, they also calculated the neutral fraction produced in the ground state, F_1^0, and showed (for the spherically symmetric $l = 0$ states) that the neutral fraction of the total beam in the excited level n is $F_n^0 = F_1^0/n^3$ for $v_p \gg v_0$. The results of the latter calculation show that the neutral yield should decrease approximately as E_p^{-4} for energies above approximately 200 keV.

In principle, both processes described in Refs. 6 and 7 can be taking place. It will be seen later that neither process can, by itself, explain the experimental results. We also shall see that whereas a large change in the density of conduction electrons has a large effect on the predictions of the above theories, the experimental differences in the neutral fraction from, say, gold $(n_0 \approx 6 \times 10^{22})$ and carbon $(n_0 \approx 3 \times 10^{18})$[11] are minor. Therefore, some other mechanism must be operative in the case of semimetals or insulators, and may also dominate the capture process in metals.

Recently, McLelland[8] has proposed a model that is applicable only when the conduction-electron density is low, as in semimetals and insulators: Within the material, a fast proton produces a shower of positive-energy electrons, some of which have velocities close to that of the proton and thus are candidates for possible capture. As these are free electrons, an interaction via the lattice potential is required for the capture process to take place. After making plausible choices of the free-electron yield and energy-distribution function, McLelland calculated capture probabilities for a carbon target that are in order-of-magnitude agreement with experiment. The numerous assumptions required to obtain quantitative results limit the usefulness of these calculations; however, the general features of the model can be tested by comparing the calculated and experimental energy dependence. These calculations were carried out for proton energies above 20 keV, and included a

n^{-3} distribution over excited states.

There is, of course, the approach introduced by Bohr and Lindhard, considering a solid as a thick target of isolated atoms.[12,10] In this spirit we will compare equilibrium fractions from solid and gaseous magnesium targets in Sec. IV.

III. APPARATUS AND PROCEDURE

A beam of deuterium ions from an electrostatic accelerator was momentum analyzed and entered the charge-exchange and analysis chamber (Fig. 1). After collimation to a diameter of 1.57 mm, the beam, typically 1 μA, passed through a 6-mm-diam self-supporting target foil.

The beam that emerged from the foil consisted of positive and negative deuterium ions and neutral atoms in various states of excitation. The two charged states were separated by electrostatic deflection and stopped in 2.25-cm-diam magnetically guarded Faraday cups. The neutral component was detected by measuring the power of a 2.25-cm-diam pyroelectric detector,[13] or, at the lowest energies where the current and power were small, by measuring the current from a 2.25-cm-diam surface-barrier solid-state detector that was operated as an ion chamber. In either case, the neutral detectors were calibrated by switching the beam deflection voltage off, thereby putting the known charged components into the neutral detector. The outputs of the various detectors were amplified and integrated. A block diagram of the general electronic circuitry is shown in Fig. 2. A calibration of the detectors and measurement of the fractions in various charge states required about 30 sec, a time very much shorter than any observed time constant associated with contamination of the foil surfaces.

The energy of the deuterons emerging from the foil was analyzed by electrostatic deflection into a Faraday cup masked by a plate with a 3-mm-wide slit.

Two methods were used to determine the fractions of the neutral beam that emerged in highly excited levels. The first was an optical method that had previously been used to determine yields from charge exchange in a magnesium vapor target and gave information about the population of the $n = 6$ levels.[14] The second was electric field ionization of atoms in highly excited levels[15] ($12 \le n \le 18$). These two methods will be described in greater detail further on in this section.

The target foil consisted of a 6-mm-diam, 5-10-μg/cm^2 carbon foil substrate.[16] The energy loss in the substrate was usually 2 to 5 keV. The presence of deuterons whose energy had not been degraded by this amount was an indication that there were pinholes in the substrate. If this occurred, the foil was moved until the fraction of primary energy
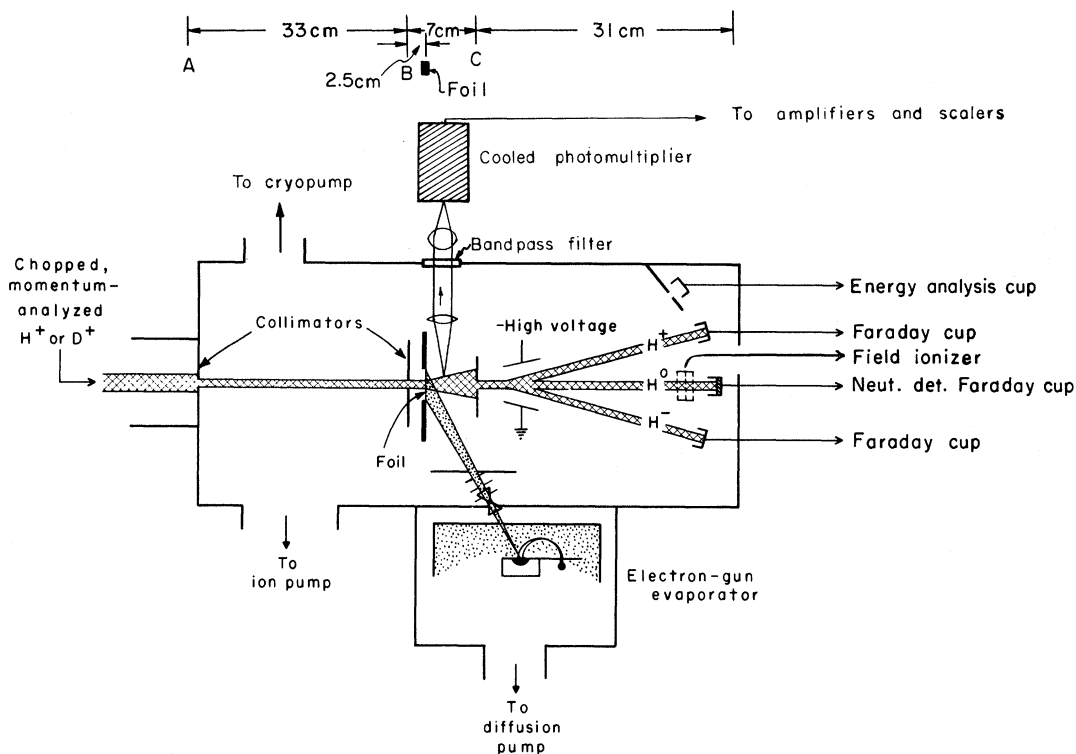
FIG. 1. Analysis chamber. Insert shows collimation: A, 1.32; B, 1.57; C, 2.72 mm diameter.

deuterons was less than 10^{-4}.

Fresh material could be evaporated onto the substrate while the target chamber was maintained at high vacuum. To accomplish this, an electron-gun (e-gun) evaporator unit was mounted in a separately pumped vacuum chamber which was connected to the target chamber by means of an elec-

trically operated valve. This valve, which was normally closed, was used as a shutter to control the amount of material deposited on the foil. The procedure was to outgas the material in the evaporator and open the shutter to expose the foil while the beam was passing through it. When enough material had been deposited to degrade the energy
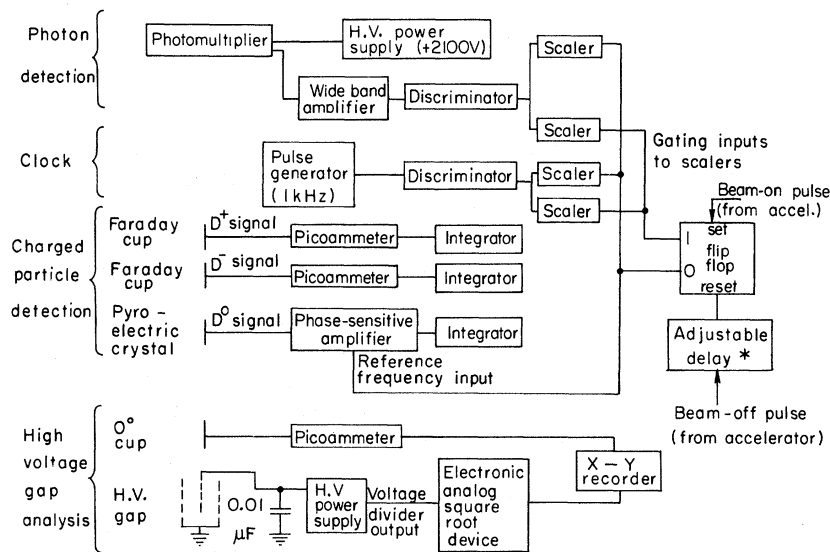
FIG. 2. Block diagram of the electronics.

*Delay adjusted until beam-gate covers entire beam-on period

of the emerging beam by several hundred eV, the shutter was closed and the charge fractions were measured. This procedure was repeated until the measured charge fractions no longer changed; this usually occurred after an energy loss of about 2 keV. Once equilibrium was attained a complete set of measurements was taken.

Every attempt was made to achieve a clean high vacuum. Metal gaskets were used everywhere except in three valves which had Viton O rings. The chamber was baked with a quartz lamp mounted inside the vacuum system. The system was roughed out with N_2 aspirators and sorption pumps, routinely maintained at low pressures ($\approx 5 \times 10^{-8}$ Torr) by a VacIon pump, and during measurements involving evaporation was maintained at 2×10^{-9} Torr by a liquid-helium cryopump. When the shutter was opened, the pressure usually rose to as much as 3×10^{-8} Torr, but quickly pumped down again as soon as the shutter was closed.

Two Ti-getter pumps in the beam line and a small aperture (A in Fig. 1) isolated the high-vacuum chamber from the relatively high-pressure (10^{-5}- to 10^{-6}-Torr) accelerator section. The foil substrates were introduced through a vacuum lock so that foils could be changed without bringing the entire system up to air.

In the optical method of detecting excited atoms, single photons from the 4101-Å transition (Balmer H_6) from the $n = 6$ level were counted. At first a monochromator was used to select the proper spectral line, but during most of the experiment we used a bandpass filter. To maximize the light focused on the photomultiplier, the first lens of the system was in a reentrant cavity in the analysis chamber, 5 cm from the beam line. An EMI type 6256S photomultiplier, cooled to $-20\,°C$ to eliminate background noise, was used to detect the photons.

The optical detection efficiency was measured each time the foil or energy was changed, and after each evaporation. This was accomplished by introducing nitrogen at four gas pressures from 2 to 9 μTorr into the analysis chamber and counting photons from the N_2^+ transition with the band head at 3914 Å [0-0 band of the first negative band system of N_2^+ ($B\,^2\Sigma_u - X\,^2\Sigma_g$)], for which the yields produced by either proton or hydrogen-atom impact have been measured by several groups (see Appendix A). The pressure was measured with an ionization gauge which was calibrated with a Barocel capacitance manometer in the 10^{-4}–10^{-5}-Torr range. Following a scan with a monochromator to determine the band intensity as a function of wavelength, the light from this transition was selected with a second bandpass filter. The relative transmission of the filters, windows, and lenses for the H_6 line and the N_2^+ band, measured independently, was

used to obtain the optical efficiency at 4101 Å. The transmission measurements were confirmed by comparing ratios of H_6 and 0-0 band N_2^+ counts made simultaneously with the monochromator and filters. (In the process, we showed, by scanning the 0-0 band with a narrow slit, that $\gtrsim 95\%$ of the N_2^+ light was passed by the slit used in the experiments. The difference in photon counting efficiencies, using the monochromator at the hydrogen and nitrogen wavelengths, was estimated to be 5%).[14]

The technique for obtaining the yield of atoms in the $n = 6$ level from the measured counting rates is essentially the same as described in Ref. 14; however, additional information about the nitrogen excitation cross sections has become available and is included here. The way that these data are combined, the method of reducing data, and a brief description of error estimates are given in Appendix A. Additional information can be obtained from Ref. 14. The main sources of uncertainty in this method are the unknown population distribution of the substates of $n = 6$ (we assume a statistical distribution here[17]) and the nitrogen excitation cross section. Our estimate of the latter is about $\pm 30\%$ (see Appendix A); the total absolute standard error is estimated to be about $\pm 40\%$. However, the relative standard errors, based on repeatability, are estimated to be approximately $\pm 15\%$.

The polarization of the light from hydrogen decays and nitrogen excitation was checked and found to be small, less than 4% for 25- to 60-keV deuterons. (We have found previously that the polarization of the H_6 radiation from electron capture in magnesium vapor targets is also negligible.[14])

The excited-state measurements made with the electric field ionization technique were carried out with a high-voltage gap made of three 22-mm-diam, 8-line/cm, 96% transparent tungsten mesh grids spaced 3 mm apart on the entrance side and 8 mm apart on the exit side. The pyroelectric detector, which in this case served as a magnetically shielded Faraday cup, was used to detect the ions produced in the gap. The center grid could be operated at voltages up to ± 15 kV, which is enough to ionize part of the $n = 11$ level. For convenience, the maximum voltage was usually ± 9 kV, sufficient to ionize most of the $n = 12$ level. The minimum useful voltage, and therefore the maximum measurable n level, was set by the electric field between the beam deflection plates, which varied with energy. Most of the results quoted later are for n values approximately between 12 and 18.

A plot of the ion current vs the square root of the gap voltage was made on an X-Y recorder. As described in Appendix B, the slope of the line obtained in this way is approximately proportional to the excited-state yield, and the absolute yield can be obtained from knowledge of the lifetime of atoms

in the electric field and absolute values of the field strength. The method of data analysis and uncertainty estimation is outlined in Appendix B. Standard errors based on reproducibility are estimated to be about ±15%. The absolute standard error to be assigned to the measurements obtained with this technique is difficult to assess, because of the lack of knowledge about the n dependence of the population of the levels at low energies (Appendix B). Our estimate is ±30%.

IV. RESULTS

The experimental results are presented in two ways: graphs for carbon and magnesium, in order that the typical scatter in individual points and the comparison among various experiments will be apparent; and tabulations for all of the materials at several energies, obtained from smooth lines drawn through the experimental points. When material was evaporated onto the substrate, the results characteristic of that material were obtained. No appreciable temporal variations of either charge or excited-atom fractions occurred after evaporation under normal data-collection conditions ($\sim 2 \times 10^{-9}$ Torr). However, at a higher pressure, 1×10^{-8} Torr, temporal variations could be measured easily for low ion energies. By far the largest change occurred with a Mg surface. As an example, for deuterons with an exit energy of 8 keV, the excited-atom fraction increased at a rate of about 3%/min following the evaporation, and the F$^-$ fraction decreased at a somewhat slower rate (presumably due to contamination of the foil surface). In time (sometimes several hours at 2×10^{-9} Torr) all surfaces acquired the characteristics of a carbon foil prior to evaporation (a "dirty" carbon foil).
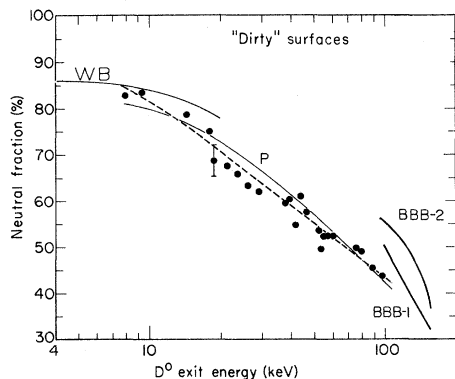

FIG. 3. Neutral fractions from "dirty" surfaces. P (Ref. 2); WB (Ref. 18); BBB-1(C) and BBB-2(Al) (Ref. 19); ● (present work) (a representative standard error is shown). The H atom results of Refs. 2, 18, and 19 have been plotted at twice the H energy. The dashed line is drawn through our data.
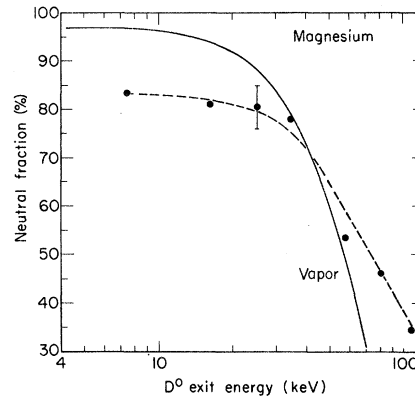

FIG. 4. Neutral fraction from a fresh Mg surface. The estimated standard error is shown at a representative point. The dashed line is drawn through our data. The solid line is the neutral fraction obtained from a thick Mg vapor target (Ref. 20).

A. Total Neutral Fraction

The measured total (all n values) yields of neutral deuterium atoms exiting from "dirty" C and fresh Mg surfaces are shown in Figs. 3 and 4; Table I contains the yields for all targets. Our estimated standard error in these measurements is ±5%. The "dirty" surface results are seen to be in reasonable agreement with the earlier measurements by Phillips,[2] by Wax and Bernstein,[18] and by Berry et al.[19]

We could detect no significant difference in the neutral fraction between "dirty" or freshly evaporated carbon films. Gold is the only other material for which a comparison with a previous measurement (by Phillips) is possible; these results also agree within the estimated uncertainties.

Also shown in Fig. 4 are the thick-target Mg vapor results of Moses and Futch.[20]

B. Negative Fraction

The fraction of the incident beam that emerges as D$^-$ ions is shown for carbon and magnesium surfaces in Figs. 5 and 6. Averaged values for all of the materials are given in Table I. There is a small difference between yields from "clean" and "dirty" carbon surfaces below 40 keV. The "dirty" carbon data are in general agreement with the earlier data of Phillips. The curves for Nb and Au (not shown graphically) are very much like the carbon data, the yields from all of these being much smaller than from Mg at energies below about 30 keV. Our estimated standard error of these measurements is ±10%. Our gold data agree very well with those of Phillips at energies of 50 keV and higher, but are about 30% lower than Phillips's data at lower energies. Also shown in Fig. 6 are

TABLE I. Charge fractions for deuterium beams emerging from various surfaces. The estimated standard errors are ±5% for F^0 and ±10% for F^-. The entries were obtained from smooth curves drawn through the data, as in Figs. 3–6.

Exit energy	"Dirty" C		C		Mg		Nb		Au	
(keV)	F^0	F^-	F^0	F^-	F^0	F^-	F^0	F^-	F^0	F^-
8	0.84	0.038	0.80	0.024	0.83	0.120	0.90	0.037	...[a]	0.028[b]
16	0.75	0.024	0.76	0.185	0.82	0.090	0.85	0.030	...	0.027[b]
30	0.64	0.016	0.67	0.0140	0.78	0.035	0.73	0.015	...	0.020[b]
50	0.55	0.0112	0.56	0.0105	0.65	0.0143	0.55	0.0067	0.67	0.0120
70	0.50	0.0081	0.50	0.0081	0.53	0.0080	0.44	0.0046	0.59	0.0076
100	0.43	0.0053	0.44	0.0053	0.38	0.0042	0.38	0.0030	0.40	0.0037

[a]The large angular scattering in Au at low energies resulted in such low signals that no reliable F^0 measurements were obtained.

[b]Derived from measured D^+ and D^- currents and F^0 from Phillips (Ref. 2).

the thick-target Mg *vapor* results of Moses and Futch.[20]

C. Excited-Atom Fraction

The basic assumption in the analysis of the electric field ionization data is that the excited-atom population has an n^{-3} dependence on the principal quantum number (see Appendix B). The excited-atom results are therefore presented in the form $n^3 F_n$, where F_n is the ratio of the number of atoms in the principal quantum level n to the total number of particles in the beam (charged and neutral). In this presentation one can readily compare our optical measurements for the $n = 6$ level, our field

ionization measurements for the levels $n \approx 12$ to 18, and the field ionization measurements of Sweetman *et al.*[3] for $n = 11$. The results are presented graphically for "dirty" C and fresh Mg surfaces in Figs. 7 and 8. For a comparison of the different foil materials we present the field ionization results in Table II.

As discussed in the Appendixes, the standard errors are estimated to be about ±40% for the optical measurements and ±30% for the field ionization measurements. Only the relative standard errors, based on reproducibility, are shown in Figs. 7 and 8.

Also shown in Fig. 8 are the field ionization results ($n \approx 9$ to 15) for Mg *vapor* reported by Il'in
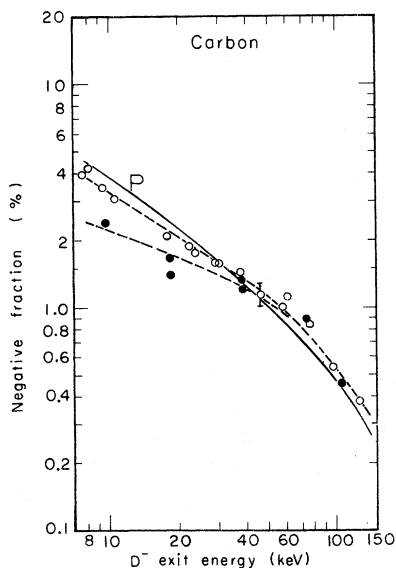

FIG. 5. Negative fraction from a carbon foil: ● ("dirty" carbon); O (freshly evaporated carbon). The estimated standard error is shown at a representative point. The dashed lines are drawn through our data. The line labeled P represents the H^- results of Phillips (Ref. 2) for dirty surfaces, plotted at twice the H^- energy.
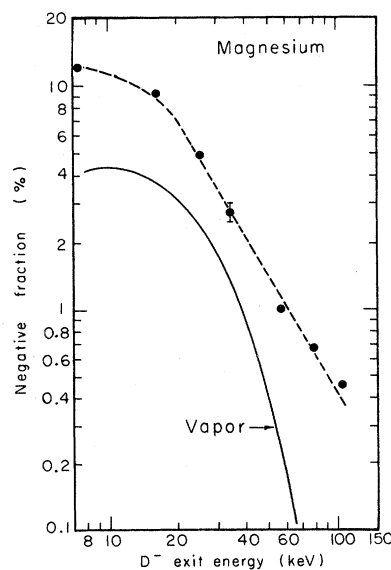

FIG. 6. Negative fraction from a fresh Mg surface. The estimated standard error is shown at a representative point. A dashed line is drawn through the data. The solid line is the negative fraction obtained from a thick Mg vapor target (Ref. 20).
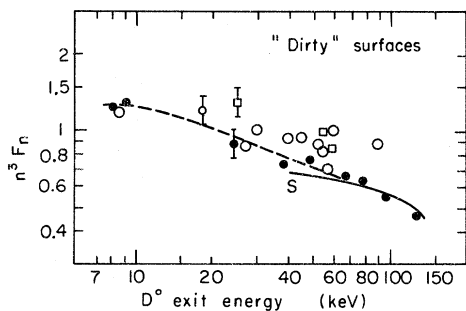
FIG. 7. Excited-atom results for "dirty" carbon surfaces, presented in the form n^3F_n, where F_n is the ratio of the number of atoms in the principal quantum level n to the total number of particles in the beam (charged and neutral). Optical method (this work):○ (filter); □ (monochromator). Field-ionization measurements: ● (present work); solid line (Sweetman et al., Ref. 3). The representative standard errors indicated are based on reproducibility only. The estimated standard errors in the absolute values are ±30% for the field ionization and ±40% for the optical results. The dashed line is drawn through our field-ionization data.

FIG. 8. Excited-atom results, n^3F_n, for fresh Mg surfaces:○ (filter); ● (field ionization). The representative standard errors indicated are based on reproducibility only. The estimated standard errors in the absolute values are ±30% for the field ionization and ±40% for the optical results. The dashed line is drawn through our field-ionization data. The solid lines are for Mg vapor targets:vapor 1 (thick target, Ref. 21); vapor 2 (target optimized for maximum excited–atom yield, Ref. 21).

et al.[21]

V. DISCUSSION AND CONCLUSIONS

A. Neutral Fraction F^0

Where our data overlap, they are in good agreement with those of Phillips[2]; our measurements were made at pressures several orders of magnitude lower than his.

Measured neutral yields from solid Mg and Au surfaces are shown in Fig. 9, together with theoretical predictions from Refs. 6 and 7 (negative-ion formation is neglected). The calculated results, using the various theoretical approximations, bracket the experimental data and could be combined empirically to approximate the experimental curves.

The experimental neutral yield from carbon is not very different from the metallic yields (see Table I). Since carbon has a much lower free-electron density than the metals, the models of Refs. 5 and 6 cannot be applicable. As mentioned in Sec. II, the parameters in McLelland's electron-shower model for carbon[8] can be adjusted to give approximate agreement with experiment in the proton energy range from about 20 to 70 keV. However, it seems premature to consider this as verification of the correctness of the model.

In Fig. 4 we included, for comparison with the results for a solid Mg target, an experimental curve of F^0 vs energy for a thick magnesium *vapor* target. One sees that the data from the two types of target are quite different. Nevertheless, in the energy range of the present experiment it is a fair working approximation to treat the solid targets as
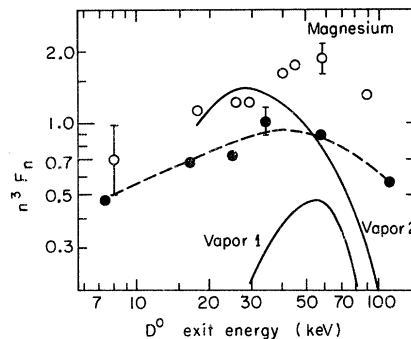
if they were thick gas targets. Discussion of some of the differences observed and expected for targets in the different phases, as related to stopping power, can be found in the literature.[22]

B. Negative Fraction F^-

Our results for F^- are in good agreement with the measurements of Phillips[2] for the two materials (Au and "dirty" surfaces) common to both experiments. We are not aware of any theoretical estimates with which to compare our results.

There is little difference in the negative fractions produced from C, Nb, Au, or "dirty" surfaces for the energy range covered in this experiment (see Table I). Mg, however, produces a significantly larger fraction of D⁻ below 50 keV. Vapor targets

TABLE II. Excited–atom yields, expressed as the product of n^3 and F_n (the fraction of the total beam in the level n), for deuterium beams emerging from various surfaces. These results are obtained using electric field ionization of levels $n \approx 12$ to 18. The relative standard errors, based on reproducibility, are ±15% except at 8 keV, where they are ±30%. The standard errors in the absolute values are estimated to be ±30%, except at 8 keV, where they are ±45%.

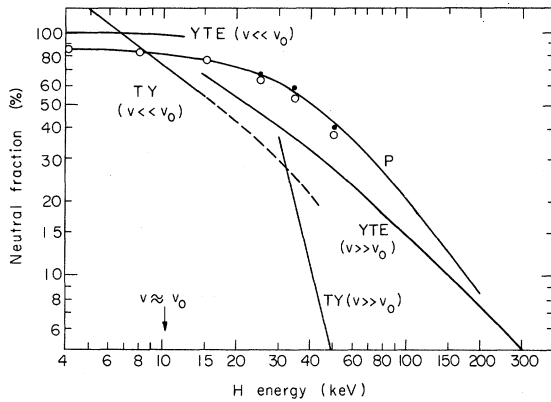| Exit energy (keV)	"Dirty" carbon	C	Mg	Nb	Au
8	1.27	0.85	0.51	0.40	0.52
16	1.09	1.09	0.69	0.54	0.52
30	0.86	0.86	0.90	0.74	0.57
50	0.71	0.71	0.90	0.88	0.59
70	0.63	0.63	0.80	0.82	0.62
100	0.55	0.55	0.64	0.63	0.59

FIG. 9. Comparison of measured neutral yields from solid Mg ($\bullet$) and Au ($\bigcirc$) surfaces with theoretical predictions from YTE (Ref. 6) and TY (Ref. 7). The solid line P is Phillips's Au data (Ref. 2). Our experimental results with deuterium are plotted at half-energy.

of low-ionization-potential materials (such as alkali or alkali-earth metals) are known to yield relatively large fractions of negative ions at low energies.[23] From Fig. 6 we see that F^- from a Mg surface exceeds that from a thick Mg vapor target.

C. Excited-Atom Fractions

As the data in Figs. 7 and 8 indicate, both for "dirty" C and fresh Mg surfaces the excited-atom fractions obtained with the optical method exceed the field ionization results. The difference in the results of the two methods is more pronounced for Mg, but even in this case the fractions agree within the estimated standard errors ($\pm 40\%$ for optical and $\pm 30\%$ for field ionization).

Since the optical results are for the level $n = 6$ and those from field ionization are for $n \simeq 12$ to 18, the general agreement of the measurements supports our assumption of an n^{-3} scaling law for the population of the level n. The theories of both McLelland[8] and of Trubnikov and Yavlinskii[7] predict this n^{-3} dependence at high energies; however, there is no quantitative agreement between either of these calculations and the experimental results.

As was the case for F^0 and F^-, the energy dependence of the excited-atom fraction from solid Mg is quite different from that produced in a Mg vapor target. This is demonstrated in Fig. 8, where we have indicated the field ionization ($n \approx 9$ to 15) results of Il'in et al.[21] for both the equilibrium (thick-target) yield and the optimum yield, which occurs at a lower target thickness.

For clean surfaces the excited-atom fractions exhibit a decrease both at the high- and low-energy end of our energy range. The fraction produced in "dirty" carbon, on the other hand, continues to increase with decreasing energy.

APPENDIX A: ANALYSIS OF OPTICAL DATA

Neutral atoms emerging from the foil travel 1.28 cm before entering a region 1.5 cm long (along the beam line) that is imaged on the photomultiplier cathode. Some of the deuterium atoms that emerge from the foil in the $n = 6$ level decay before they reach the region of observation, some of the remainder decay within the 1.5-cm region of observation. We can assume that repopulation from higher levels (cascading) is negligible (see Ref. 14). Only those atoms in the $6s$, $6p$, and $6d$ states make the 4101-Å transitions that are recorded. To deduce the number of $n = 6$ atoms leaving the foil, we must make assumptions about the initial population distribution of angular momentum states, calculate the transition rates for the various states, and calibrate the overall optical efficiency of the system. Then from the observed photon counts, we calculate the number of atoms that were originally in the $6s$, $6p$, and $6d$ states; to these must be added the inferred number of atoms that were created in higher angular momentum states of the $n = 6$ level. If we assume that the states of the $n = 6$ level initially have a statistical $(2l + 1)$ distribution,[17] we obtain the following expression for $N(D_6)$, the measured number of photons per incident beam particle:

$$N(D_6) = N_6^0 \sum_{l=0}^{2} \frac{2l+1}{36} \exp[-v^{-1} x_1 A(6l)]$$
$$\times \frac{A(6l \to 2sp)}{A(6l)} \{1 - \exp[-v^{-1} x_2 A(6l)]\},$$

where N_6^0 is the fraction of the total incident beam that is in the level $n = 6$ at the exit of the foil, x_1 is the distance from the foil to the observation region, x_2 is the length of the observation region, v is the speed of the atoms, and

$$A(6l) \equiv \sum_{l'n'} A(6l \to n'l')$$

is the transition probability for going to all possible states. Using the decay data in Table II of Ref. 14, we obtain

$$N_6 = N(D_6) \times 10^3 (46.8 E^{-1/2} - 23.7 E^{-1})^{-1} \epsilon^{-1},$$

where ϵ is the efficiency for detecting a 4101-Å photon emitted in the observation region and E is the deuteron energy in keV.

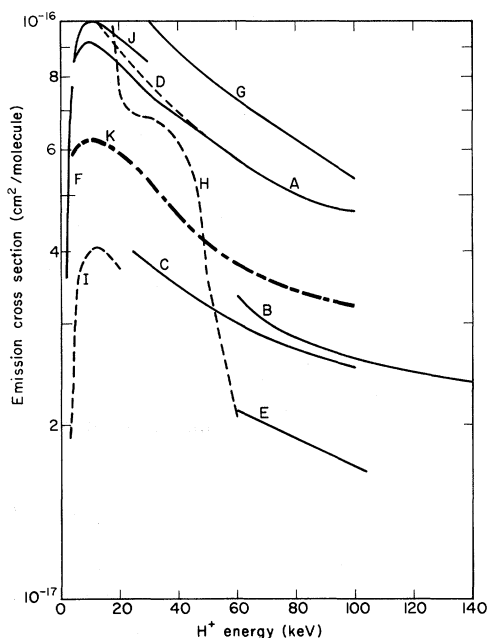In the work of Ref. 14 it was sufficient to deter-

FIG. 10. Emission cross-section measurements of
the 0-0 first negative band of N_2^+ (3914 Å) produced by
bombardment of N_2 by H^+. Solid lines indicate absolute
measurements, dashed lines indicate relative measure-
ments. A : Ref. 24; B: Ref. 25; C : Ref. 26; D : Ref. 27;
E : Ref. 28; F : Ref. 29; G : Ref. 30; H : Ref. 31; I : Ref.
32; J: Ref. 33; K: weighted average curve used in present
experiment.

mine the optical efficiency at one energy. In the
present experiment, however, there was consider-
able angular scattering of the beam by the foil,
which depended on the beam energy, foil material,
and foil thickness. This meant that whereas the
photomultiplier, which viewed the beam near the
exit of the foil, received light from the entire
beam, the charge detectors received only that part
of the beam that passed through the collimator D
(Fig. 1). Consequently, the optical efficiency in
this experiment is the number of detected photons
per *detected* particle. The efficiency was deter-
mined for each measurement. As described in
Sec. III, the method of obtaining ϵ is straightfor-
ward and the result contains no large uncertainties
other than those in the cross sections for excitation
of the calibration band at 3914 Å by deuterons and
deuterium atoms in N_2 gas. (In the absence of any
other information, we assume that the few negative
deuterium ions have the same excitation cross sec-
tions as D^+ ions.) Measurements of these cross
sections reported during the past 12 years[24-33] are
shown in Figs. 10 and 11 for incident protons and
hydrogen atoms, respectively. (It has been shown
by Thomas *et al.* that hydrogen cross sections are
the same as for deuterons of twice the energy.[28])
Overlaying the curves in Fig. 10 shows that all but

one have the same shape, which we show in our
average curve K. The position of this average
curve was determined by obtaining a weighted geo-
metric mean of the other data at 60 keV (curve H
was not used in the average). These data points
were weighted as the inverse square of the percent-
age errors quoted by the original authors. This
gives an uncertainty in the H^+ cross section of
$\pm 29\%$ for a 68% confidence interval.

To obtain the emission cross section for H^0 im-
pact we deduced an average energy dependence by
overlaying the curves in Fig. 11. Since we know
of only two absolute measurements in this case, the
following procedure was used to determine the
magnitude of the cross section: We used the aver-
age value calculated for H^+ impact and related it to
H^0 impact by dividing it by the ratio of the 60-keV
cross sections for the three groups who published
data for both processes at this energy. This aver-
age ratio was 1.52, so the average curve for H^0
impact is normalized to 2.49×10^{-17} cm^2/molecule
at 60 keV.

The uncertainty in the H^+ cross section, using a
68% confidence interval, is $\pm 29\%$. To obtain the
uncertainty in the H^0 cross section, one folds into
this the uncertainty in the ratio of cross sections
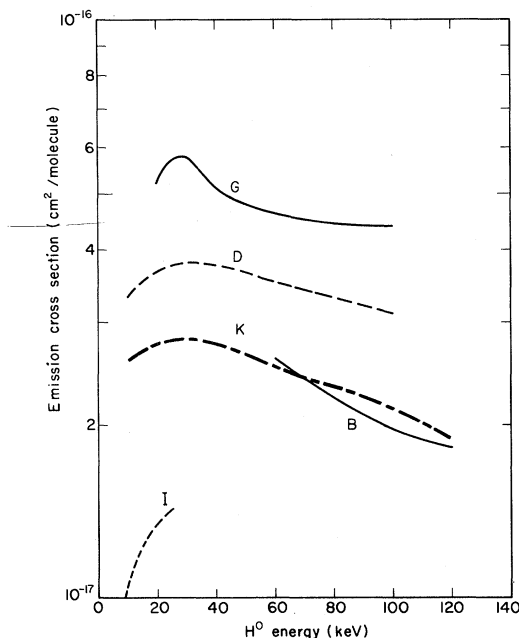($\pm 13\%$) and obtains $\pm 31\%$.

FIG. 11. Emission cross-section measurements of
the 0-0 first negative band of N_2^+ (3914 Å) produced by
bombardment of N_2 by H^0. Solid lines indicate absolute
measurements, dashed lines indicate relative measure-
ments. B : Ref. 25; D : Ref. 27; G : Ref. 30; I : Ref. 32;
K : derived cross-section curve used in present experi-
ment (see text).

APPENDIX B: ANALYSIS OF ELECTRIC-GAP DATA

A review of the technique of field ionization to measure the population of excited levels of hydrogen atoms can be found in Ref. 15. In the present experiment we used the method of Il'in et al.[34] to analyze the field-ionized proton current: The electric field required to destroy an excited level n, from the Bohr model of the atom, is $E_n = bn^{-4}$, and the population of highly excited states, from Born approximation calculations of electron capture, is given by αn^{-3}. Il'in et al. showed that these relations lead to an expression for the fraction of the atom beam which is field ionized:

$$I(E) = \alpha E^{1/2}/2b^{1/2} , \tag{B1}$$

where E is the applied electric field. Thus, by plotting I vs $E^{1/2}$, the constant α, which characterizes the excited-state yield, can be obtained from the slope.

From the calculations of Bailey, Hiskes, and Riviere[35] we find that for a statistical distribution of substates and an ionization time of 3×10^{-10} sec (a typical time of flight through our gap), $E_n = (4.3 \times 10^5)n^{-3.82}$ kV/cm. It can be shown that for our range of n there will be only a few percent difference in the results if we fit this to the classical expression $E_n = bn^{-4}$, with $b = 6.8 \times 10^5$ kV/cm. (Il'in et al. used a value $b = 6.2 \times 10^5$ kV/cm, which they deduced from their differential measurements.) Thus Eq. (B1) can be expressed as

$$I(E) = 6.1 \times 10^{-4}\alpha[E \text{ (kV/cm)}]^{1/2} . \tag{B2}$$

We used this expression to determine α.

To utilize Eq. (B2), we must relate the potential applied to the gap to the electric field. Since we use grids, the electric field in the gap is not uniform; hence we determined an equivalent electric field $E = cV$ as follows. The ion current produced in the gap exhibited a threshold behavior because the electric field in the deflection plate region pre-ionized the very highly excited states; therefore no field ionization occurred in the gap until the electric field there exceeded the deflection electric field. From this threshold we could relate the equivalent electric field in the gap to the electric field between the deflection plates, which was obtained from potential profiles in an electrolytic tank. In this way we determined that $c = 4.8 \pm 0.7$ cm^{-1}.

The estimated uncertainty in the values of α obtained in this way is made up of a random part, based on internal consistency, for which we estimate a 68% confidence interval of $\pm 15\%$, and a possible systematic error that enters through the constants b and c. By comparing our choice of b with that of Il'in et al. we assign it an uncertainty of $\pm 15\%$. Since both b and c appear in Eq. (B2) as square roots, the total systematic error in α due to these constants is $\pm 9\%$.

There is an additional uncertainty due to the assumptions involved in the model. As previously mentioned, in this analysis we assume that the populations of various quantum levels vary as n^{-3}. Hiskes's calculations for charge exchange in gases[5] show that the exponent may be closer to -4 than -3 at low energies. We do not know whether this change in n dependence also occurs for electron capture in foils. To get an indication of how a change in n dependence would affect our results, we considered three different functions for the population: n^{-3}, $n^{-3.5}$, and n^{-4}. For these the analysis leading to Eq. (B1) yields the following dependences on the gap voltage: $V^{0.5}$, $V^{0.625}$, and $V^{0.75}$. An investigation of our gap data shows that we can get an equally good fit for all three exponents over our voltage range. (On an I vs $V^{1/2}$ plot the deviation from linearity for the $V^{0.75}$ case is so slight that it might not be recognized from the data.) If we then use the different values obtained for α to evaluate the population of $n = 6$, the results are in the ratio of $1 : 0.67 : 0.44$.

†Work done under the auspices of the U. S. Atomic Energy Commission.

[1]See, for example, Nucl. Instr. Methods **90** (1970).

[2]J. A. Phillips, Phys. Rev. **97**, 494 (1955).

[3]D. R. Sweetman, A. C. Riviere, and P. Hammond, Culham Laboratory Progress Report No. CLM-PR-7, 1964, p. 47 (unpublished).

[4]See, for example, the discussion in the paper by K. H. Berkner, R. V. Pyle, and J. W. Stearns, Phys. Rev. **178**, 248 (1969).

[5]J. R. Hiskes, Phys. Rev. **180**, 146 (1969).

[6]Yu. N. Yavlinskii, B. A. Trubnikov, and V. F. Elesin, Izv. Akad. Nauk SSSR **30**, 1917 (1966) [Bull. Acad. Sci. Phys. **30**, 1996 (1966)].

[7]B. A. Trubnikov and Yu. N. Yavlinskii, Zh. Eksperim. i Teor. Fiz. **52**, 1638 (1967) [Soviet Phys. JETP **25**, 1089 (1967)].

[8]G. J. McLelland, Ph. D. thesis (University of Sydney, Sydney, Australia, 1968) (unpublished).

[9]J. D. Garcia, Nucl. Instr. Methods **90**, 295 (1970).

[10]W. S. Bickel, K. Jensen, C. S. Newton, and E. Veje, Nucl. Instr. Methods **90**, 309 (1970).

[11]Charles Kittel, *Introduction to Solid State Physics*, 4th ed. (Wiley, New York, 1971).

[12]N. Bohr and J. Lindhard, Kgl. Danske Videnskab. Selskab, Mat.−Fys. Medd. **28**, No. 7 (1954).

[13]K. H. Berkner, B. R. Myers, and R. V. Pyle, Rev. Sci. Instr. **39**, 1204 (1968).

[14]K. H. Berkner, W. S. Cooper III, S. N. Kaplan, and R. V. Pyle, Phys. Rev. **182**, 103 (1969).

[15]See, for example, A. C. Riviere, in *Methods of Experimental Physics*, edited by B. Bederson and W. L. Fite (Academic, New York, 1968), Vol. 7, Part A, Chap. 2.4.

[16]Carbon is used as a substrate material because it is strong, low Z, and easily and economically obtained. Our foils were purchased from Yissum Research Corp., Hebrew University, Jerusalem, Israel.

[17]The consequences and alternatives to choosing an initially statistical substate distribution are discussed in Ref. 14.

[18]R. L. Wax and W. Bernstein, Rev. Sci. Instr. **38**, 1612 (1967).

[19]H. G. Berry, J. Bromander, and R. Buchta, Nucl. Instr. Methods **90**, 269 (1970).

[20]K. G. Moses and Archer H. Futch, Jr., Bull. Am. Phys. Soc. **11**, 344 (1966), and private communication.

[21]R. N. Il'in, V. A. Oparin, E. S. Solov'ev, and N. V. Fedorenko, Zh. Eksperim. i Teor. Fiz. Pis'ma v Redaktskiyu **2**, 310 (1965) [Sov. Phys. JETP Letters **2**, 197 (1965)].

[22]See, for example, W. Meckbach and S. K. Allison, Phys. Rev. **132**, 294 (1965).

[23]See, for example, W. Gruebler, P. A. Schmelzbach, V. Koenig, and P. Marmier, Helv. Phys. Acta **72**, 254 (1970).

[24]J. L. Philpot and R. H. Hughes, Phys. Rev. **133**, A107 (1964).

[25]J. M. Robinson and H. B. Gilbody, Proc. Phys. Soc. (London) **92**, 589 (1967).

[26]M. Dufay, J. Desesquelles, M. Druetta, and M. Eidelsberg, Ann. Geophys. **22**, 619 (1966).

[27]D. A. Dahlberg, D. K. Anderson, and I. E. Dayton, Phys. Rev. **164**, 20 (1967).

[28]E. W. Thomas, G. D. Bent, and J. L. Edwards, Phys. Rev. **165**, 32 (1968).

[29]N. P. Carlton and T. R. Lawrence, Phys. Rev. **109**, 1159 (1958).

[30]H. A. B. Gardiner, W. R. Pendleton, Jr., J. J. Merrill, and D. J. Baker, Phys. Rev. **188**, 257 (1969).

[31]J. R. Sheridan and K. C. Clark, Phys. Rev. **140**, A1033 (1965).

[32]R. J. McNeal and D. C. Clark, J. Geophys. Res. **74**, 5065 (1969).

[33]W. F. Sheridan, O. Oldenberg, and N. P. Carlton, in Second International Conference on the Physics of Electronic and Atomic Collisions, Boulder, Colorado, 1961, p. 159 (unpublished).

[34]R. N. Il'in, B. I. Kikiani, V. A. Oparin, E. S. Solov'ev, and N. V. Fedorenko, Zh. Eksperim. i Teor. Fiz. **47**, 1235 (1964) [Sov. Phys. JETP **20**, 835 (1965)].

[35]D. S. Bailey, J. R. Hiskes, and A. C. Riviere, Nucl. Fusion **5**, 41 (1965).